Enhanced Transfection Efficiency of Multicomponent Lipoplexes in the Regime of Optimal Membrane Charge Density

Giulio Caracciolo,*,† Daniela Pozzi, and Ruggero Caminiti

Chemistry Department, University of Rome "La Sapienza", P.le A. Moro 5, 00185 Rome, Italy

Cristina Marchini,† Maura Montani, and Augusto Amici

Department of Molecular Cellular and Animal Biology, University of Camerino, Via Gentile III da Varano, 62032 Camerino (MC), Italy

Heinz Amenitsch

Institute of Biophysics and X-ray Structure Research, Austrian Academy of Sciences, Schmiedelstrasse 6, A-8042 Graz, Austria

Received: April 9, 2008; Revised Manuscript Received: June 26, 2008

Recently, membrane charge density of lipid membranes, σ_M, has been recognized as a universal parameter that controls the transfection efficiency of complexes made of binary cationic liposomes and DNA (binary lipoplexes). Three distinct regimes, most likely related to interactions between complexes and cells, have also been identified. The purpose of this work was to investigate the transfection efficiency behavior of multicomponent lipoplexes in the regime of optimal membrane charge density ($1 < \sigma_M < 2 \times 10^{-2}$ e/Å^2) and compare their performance with that of binary lipoplexes usually employed for gene delivery purposes. We found remarkable differences in transfection efficiency due to lipid composition, with maximum in efficiency being obtained when multicomponent lipoplexes were used to transfect NIH 3T3 cells, while binary lipoplexes were definitely less efficient. These findings suggested that multicomponent systems are especially promising lipoplex candidates. With the aim of providing new insights into the mechanism of transfection, we investigated the structural evolution of lipoplexes when interacting with anionic (cellular) lipids by means of synchrotron small-angle X-ray diffraction (SAXD), while the extent of DNA release upon interaction with anionic lipids was measured by electrophoresis on agarose gels. Interestingly, a clear trend was found that the transfection activity increased with the number of lipid components. These results highlight the compositional properties of carrier lipid/cellular lipid mixtures as decisive factors for transfection and suggest a strategy for the rational design of superior cationic lipid carriers.

1. Introduction

Gene carriers based on lipids or polymers, rather than on engineered viruses, constitute the latest technique for delivering genes into cells for gene therapy. Cationic liposome−DNA (CL-DNA) complexes (lipoplexes) have been shown to be promising nonviral delivery systems for gene therapy applications.[1−4] Most lipoplexes form a multilayered structure with DNA embedded within cationic lipid membranes (L_α^C phase), while hexagonal complexes (H_{II}^C phase) are more rarely observed (Figure 1).

Even though the ease of production and capability of transferring large pieces of DNA represent the most relevant advantages with respect to viral vectors, their low transfection efficiency (TE) is the main concern that remains to be solved.[5]

In part, the lack of mechanistic understanding of gene delivery by CL-DNA complexes is due to the large number of parameters involved. Among physical chemical parameters affecting activity of lipoplexes, the membrane charge density (i.e., the average charge per unit area of the lipid membrane, σ_M) has recently been identified as a universal parameter that controls the TE behavior of lamellar binary lipoplexes (whose cationic membrane is a binary lipid mixture) in vitro.[6,7] In particular, the existence of an optimal membrane charge density, σ_M*, was demonstrated,[7] and TE data were found to merge onto a universal, bell-shaped curve as a function of σ_M. This bell curve

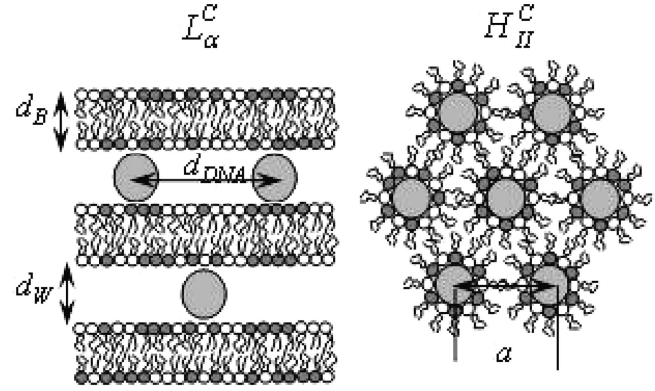

Figure 1. Schematics of the inner structure of lamellar and hexagonal CL-DNA complexes. In the lamellar phase, L_α^C, composed of alternative lipid bilayers and DNA monolayers, the lamellar repeat spacing is given by $d = d_W + d_B$. The hexagonal phase, H_{II}^C, is composed of cylinders consisting of DNA coated with a lipid monolayer arranged on a hexagonal lattice.

* To whom correspondence should be addressed. Phone: (+39)06-49913076. Fax: (+39)06-490631. E-mail: g.caracciolo@caspur.it.

† Authors contributed equally to the work.

10.1021/jp803077n CCC: $40.75
Published on Web 08/16/2008

lead to the identification of three distinct regimes, most likely related to interactions between complexes and cells: at low σ_M ($\sigma_M < 10^{-2}$ e/Å^2), TE increases with increasing σ_M; at intermediate σ_M, TE exhibits saturated behavior; at high σ_M ($\sigma_M > 2 \times 10^{-2}$ e/Å^2), TE decreases with increasing σ_M.

In a recent paper[8] we have investigated the structure−activity relationship of multicomponent lipoplexes, incorporating from three to six lipid species, in the regime of low σ_M. We found that TE data points merged onto a single experimental Gaussian curve, but striking differences with the findings of Ahmad et al.[7] emerged: (i) the optimal membrane charge density ($\sigma_M^* \sim 9 \times 10^{-3}$ e/Å^2) was much lower than that reported ($\sigma_M^* \sim 17 \times 10^{-3}$ e/Å^2); (ii) the extension of the optimal transfection regime ($w \sim 5 \times 10^{-4}$ e/Å^2) was found to be about 10-fold lower than that reported by Ahmad et al. ($w \sim 6 \times 10^{-3}$ e/Å^2); (iii) high TE can be achieved with multicomponent complexes at low membrane charge density. The latter finding was unprecedented since it had never before been achieved with binary lipoplexes. Thus, we asked ourselves whether transfection changed in the optimal transfection regime ($1 < \sigma_M < 2 \times 10^{-2}$ e/Å^2) if mediated by multicomponent lipoplexes rather than by binary complexes.

With the aim of providing insights into the mechanism of transfection, we also investigated the structural evolution of lipoplexes when interacting with anionic (cellular) lipids by means of synchrotron small-angle X-ray diffraction (SAXD), while the extent of DNA release upon interaction with anionic lipids was measured by electrophoresis on agarose gels.

2. Experimental Methods

2.1. Liposomes Preparation. Cationic 1,2-dioleoyl-3-(trimethylammonio)propane (DOTAP) and 3β-[*N*-(*N*′,*N*′-dimethylaminoethyl)carbamoyl]cholesterol (DC-Chol), neutral dioleoylphosphatidylethanolamine (DOPE), dioleoylphosphocholine (DOPC), 1,2-dilauroyl-sn-glycero-3-phosphocholine (DLPC), 1,2-dimyristoyl-sn-glycero-3-phosphocholine (DMPC), and anionic dioleoylphosphatidic acid (DOPA) were purchased from Avanti Polar Lipids (Alabaster, AL) and used without further purification. DOTAP-DOPC (A), DC-Chol-DOPE (B), DOTAP-DLPC (C), and DC-Chol-DMPC (D) CLs were routinely prepared.[9] In brief, each binary mixture, at a molar ratio of neutral lipid in the bilayer Φ = (neutral lipid/total lipid) (mol/mol) = 0.25, was dissolved in chloroform, and the solvent was evaporated in vacuum for 48 h. The obtained lipid films were hydrated with the appropriate amount of Tris-HCl buffer solution (10 mM, pH 7.4) to achieve the desired final concentration (~20 mg/mL for X-ray samples and 1 mg/mL for transfection experiments). The solutions were incubated at 30 °C for 6 h to allow for the formation of CLs. The obtained liposome solutions were then stored at 30 °C for 24 h to achieve full hydration.[10] The same protocol was followed to prepare anionic liposomes (ALs) made of DOPA.

2.2. Lipoplex Preparation. Calf thymus Na-DNA was purchased from Sigma (St. Louis, MO). DNA was dissolved in Tris-HCl buffer and was sonicated for 5 min, inducing DNA fragmentation with a length distribution between 500 and 1000 base pairs, which was determined by gel electrophoresis. Lipoplexes were prepared by mixing 100 μL of calf thymus DNA at 5.3 mg/mL with suitable volumes of liposome dispersions.

Multicomponent lipoplexes were prepared as elsewhere described.[9] For instance, premixed DOTAP-DOPC and DC-Chol-DOPE CLs loaded with DNA result in DOTAP-DC-Chol-DOPC-DOPE/DNA complexes.

TABLE 1: Lipid Composition, Molar Fraction of the *i*th Lipid Species in the Lipid Bilayer, X_i ($\sum_{i=1}^{6} X_i = 1$) and Membrane Charge Density, σ_M, of Lipoplexes Used[a]

lipoplex	X_{DOTAP}	$X_{DC\text{-}Chol}$	X_{DOPC}	X_{DOPE}	X_{DMPC}	X_{DLPC}	σ_M 10^{-2} (e/Å^2)
A	0.75	0	0.25	0	0	0	1.09
A−C	0.75	0	0.125	0	0	0.125	1.10
C	0.75	0	0	0	0	0.25	1.12
A−B (4:1)	0.6	0.15	0.2	0.05	0	0	1.21
A−B (3:1)	0.56	0.19	0.19	0.06	0	0	1.24
C−D	0.375	0.375	0	0	0.125	0.125	1.37
A−B	0.375	0.375	0.125	0.125	0	0	1.38
A−B (1:2)	0.25	0.5	0.08	0.17	0	0	1.47
A−B (1:5)	0.125	0.625	0.04	0.21	0	0	1.57
D	0.	0.75	0	0	0.25	0	1.62
B−D	0	0.75	0	0.125	0.125	0	1.65
B	0	0.75	0	0.25	0	0	1.67

[a] Samples are listed as a function of increasing σ_M. Where not specified, cationic liposomes were mixed in equimolar ratio.

In Table 1 the multicomponent lipoplexes are listed as a function of increasing membrane charge density, σ_M, that was calculated according to the literature.[8] The molar fraction X of each lipid species in the lipid bilayer is also specified.

All samples were prepared with the same cationic lipid/DNA ratio (mol/mol), i.e., ρ = (cationic lipid (by mole)/DNA base) = 2. After storage for 3 days at 4 °C, allowing the samples to reach equilibrium,[10] they were transferred to 1.5 mm diameter quartz X-ray capillaries (Hilgenberg, Malsfeld, Germany). The capillaries were centrifuged for 5 min at 6000 rpm at room temperature to consolidate the samples.

2.3. Lipoplex/Anionic Liposome System Preparation. Lipoplexes and anionic liposomes made of DOPA were mixed at different anionic/cationic charge ratios *R*. These mixed dispersions were then equilibrated for 2 days, filled into quartz capillaries, and flame-sealed. Final concentration of samples was 10 mg/mL. To ensure equilibration, the samples were kept at 4 °C for 2 days.

2.4. Transfection Efficiency Experiments. Cell lines were cultured in Dulbecco's modified Eagle's medium (DMEM) (Invitrogen, Carlsbad, CA) supplemented with 1% penicillin−streptomycin (Invitrogen) and 10% fetal bovine serum (FBS, Invitrogen) at 37 °C and 5% CO_2 atmosphere, splitting the cells every 2−4 days to maintain monolayer coverage. For luminescence analysis, mouse fibroblast NIH 3T3 cells were transfected with pGL3 control plasmid (Promega). The day before transfection, cells were seeded in 24-well plates (150 000 cells/well) using medium without antibiotics. Cells were incubated until they were 75−80% confluent, which generally took 18 to 24 h. For TE experiments, lipoplexes were prepared in Optimem (Invitrogen) by mixing for each well of 24-well plates 0.5 μg of plasmid with 5 μL of sonicated lipid dispersions (1 mg/mL). These complexes were left for 20 min at room temperature before adding them to the cells. The cells were incubated with lipoplexes in Optimem (Invitrogen) for 6 h to permit transient transfection; the medium was then replaced with DMEM supplemented with FBS. Luciferase expression was analyzed after 48 h and measured with the Luciferase Assay System from Promega, and light output readings were performed on a Berthold AutoLumat luminometer LB-953 (Berthold, Bad Wildbad, Germany). TE was normalized to milligrams of total cellular protein in the lysates using the Bio-Rad Protein Assay Dye Reagent (Bio-Rad, Hercules, CA).

2.5. Synchrotron Small-Angle X-ray Diffraction Measurements. All SAXD measurements were performed at the Austrian SAXS beamline of the synchrotron light source ELETTRA

(Trieste, Italy).[11] SAXD patterns were recorded with a gas detector based on the delay line principle covering a q range of between 0.05 and 1.5 Å^{-1}. The angular calibration of the detector was performed with silver behenate [$CH_3(CH_2)_{20}$-COOAg] whose d value corresponds to 58.38 Å. Exposure times for every sample were 100 s. No evidence of sample degradation due to radiation damage was observed in any of the samples at this exposure. The data have been normalized for primary beam intensity and detector efficiency, as well as having the background subtracted. Temperature was controlled in the vicinity of the capillary to within ±0.1 °C (Anton Paar, Graz, Austria).

2.6. Agarose Gel Electrophoresis Experiments. After equilibration, naked plasmid DNA, lipoplexes, and lipoplexes/AL systems with different R were analyzed by electrophoresis. Electrophoresis studies were conducted on 1% agarose gels containing Tris−borate−EDTA (TBE) buffer. After electrophoresis, ethidium bromide (Et-Br) was added and then visualized. Lipoplexes were prepared by mixing 40 μL of lipid dispersions (1 mg/mL, Tris-HCl buffer) with 4 μg of pGL3 control plasmid ($\rho = 2$). These complexes were allowed to equilibrate for 1 h at room temperature. Then, 10 μL of each sample were mixed with 2 μL of loading buffer (glycerol 30% v/v, bromophenol blue 0.25% v/v) and subjected to agarose gel electrophoresis for 1 h at 80 V. The electrophoresis gel was visualized and digitally photographed using a Kodak Image Station, model 2000 R (Kodak, Rochester, NY). Digital photographs were elaborated using a dedicated software (Kodak MI, Kodak) that allows calculation of the molar fraction of released DNA, X_{DNA}.

3. Results

3.1. Transfection Efficiency Results. In our previous study[8] we showed that, at low membrane charge density ($\sigma_M < 10^{-2}$ e/Å^2), multicomponent lipoplexes exhibit a transfection efficiency higher than that of binary lipoplexes usually employed for gene delivery purposes. To extend that research, we asked ourselves whether the universal transfection curve obtained by Ahmad et al.[7] changes in the optimal transfection regime ($1 < \sigma_M < 2 \times 10^{-2}$ e/Å^2) when multicomponent lipoplexes rather than binary lipoplexes are used. To address this issue, we prepared several lipoplexes varying in composition of the lipid bilayer (Table 1). Then, we performed a transient transfection assay of mouse fibroblast NIH 3T3 and observed how transfection varied.

Remarkably, as an extension of our previous results which showed the increase and a subsequent reduction of TE in the regime of low σ_M,[8] we saw an entire bell curve of efficiency (Figure 2). The resulting curve of TE vs σ_M can be described empirically by a simple Gaussian

$$TE = TE_0 \times \exp\ -[(\sigma_M - \sigma_M^*)/w]^2 \qquad (1)$$

where $TE_0 = 3.12 \times 10^7$ RLU/mg protein, $\sigma_M^* \sim 14 \times 10^{-3}$ e/Å^{-2}, $w = (13 \pm 1) \times 10^{-4}$ e/Å^{-2}.

All lipoplex formulations we tested lie in the region of optimal membrane charge density where TE mediated by binary lipoplexes is expected to be very poorly curved as a function of σ_M (Figure 2, regime II).[7] By contrast, as Figure 2 clearly shows, we found remarkable differences in TE spanning over about 2 orders of magnitude. Comparing our results with those obtained by Ahmad and co-workers, we observe that (i) TE of binary lipoplexes (A/DNA, B/DNA, C/DNA, and D/DNA) was about 1 order of magnitude lower than that previously reported, (ii) TE profile versus σ_M was not constant but is well described by a bell-shaped curve, (iii) maximum in transfection was obtained when multicomponent lipoplexes are used.

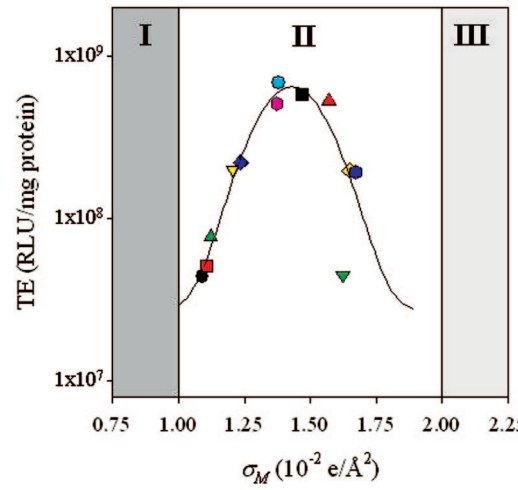

Figure 2. TE in RLU per milligram of cellular protein plotted as a function of the membrane charge density of lipid membranes, σ_M. Each symbol refers to a specific lipoplex: A (black circle), A−C (red square), C (green triangle up), A−B (4:1) (yellow triangle down), A−B (3:1) (blue diamond), C−D (pink hexagon), A−B (cyan circle), A−B (1:2) (black square), A−B (1:5) (red triangle up), B (green triangle down), B−D (yellow diamond), D (blue hexagon). Regimes of transfection are indicated according to reference:[7] low σ_M (Regime I: $\sigma_M < 10^{-2}$ e/Å^2), optimal σ_M (Regime II: $1 < \sigma_M < 2 \times 10^{-2}$ e/Å^2), and high σ_M (Regime III: $\sigma_M > 2 \times 10^{-2}$ e/Å^2).

The cationic lipid/DNA charge ratio ($\rho = 2$) as well as the molar fraction of neutral lipid in the bilayer ($\Phi = 0.25$) per sample were kept constant. Thus, only the lipid composition varies between data points.

Nevertheless, because the structure and charge ratio were the same as those reported by Ahmad et al.,[7] such physical parameters could not be taken into account to explain the observed discrepancy in the TE profile. In search of the reason why the tested formulations exhibited very different levels of transfection, we investigated the structural changes of lipoplexes upon interaction with anionic lipids. Indeed, it is well established that the structure of lipoplexes can be modified by interaction with anionic lipids, and that phase behavior of lipoplexes may control their TE.[12−17]

3.2. Structure of Lipoplexes. Synchrotron SAXD experiments revealed the nanostructure of A/DNA, A−B/DNA, and B/DNA lipoplexes at an angstrom scale with no anionic lipid added (Figure 3, $R = 0$). All lipoplexes were arranged into lamellar arrays,[18−21] (lamellar L_α^C phase, Figure 1). The sharp peaks indicated with black triangles arise from the electron density contrast normal to the lipid bilayer with lamellar periodicity $d = 2\pi/q_{001}$, which is the sum of the membrane thickness plus the thickness of the water/DNA layer. The low-intensity diffuse peak present in the SAXD patterns (marked by arrows) is due to the one-dimensional DNA interhelical spacing $d_{DNA} = 2\pi/q_{DNA}$ (Figure 1).

Figure 3 ($R = 0$) also illustrates that the 'DNA peak' position changes as a function of lipid composition. Thus, the 2D arrays of DNA molecules occupy all of the available membrane area, and the average interaxial spacing between DNA chains is fixed by the membrane charge density. The lower the membrane charge density, the larger the interhelical DNA distance.

Lamellar periodicity and DNA−DNA spacing of all multicomponent lipoplexes obtained by mixing binary CLs in different molar ratios are listed in Table 2. Table 2 shows that

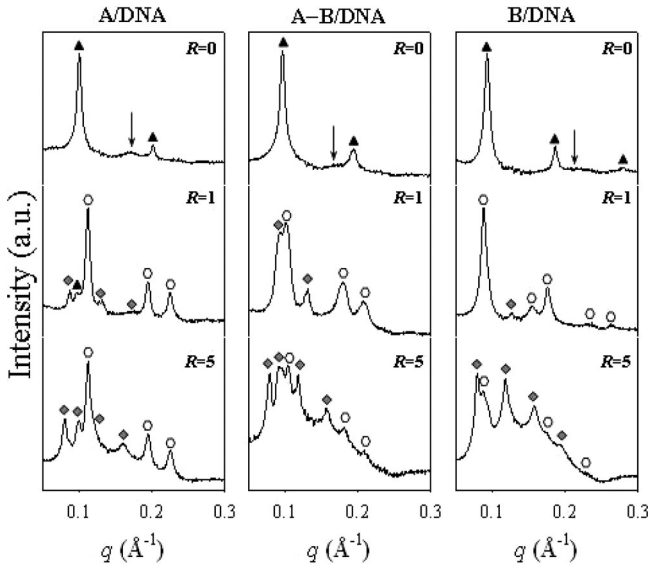

Figure 3. Representative synchrotron SAXD patterns of A/DNA/DOPA, A−B/DNA/DOPA, and B/DNA/DOPA mixtures as a function of the anionic/cationic charge ratio *R*. Bragg peaks arising from the lamellar structure of A/DNA, A−B/DNA, and B/DNA lipoplexes are indicated with black triangles. At $R = 0$, the 'DNA peak' arising from interstrand correlation is marked by an arrow. Diffraction maxima of hexagonal complexes are indicated with white hexagons, while reflections of pure DOPA are indicated with gray diamonds.

TABLE 2: Lamellar Periodicity, *d*, and DNA−DNA Spacing, d_{DNA}, of the Multicomponent Lipoplexes Investigated by SAXD[a]

lipoplex formulation	*d* (Å)	d_{DNA} (Å)
A	62.8	37.1
A−B (4:1)	63.5	37.0
A−B (3:2)	64.1	36.8
A−B	64.8	34.9
A−B (2:3)	66.2	32.1
A−B (1:4)	66.8	31.4
B	67.6	29.2

[a] Where not specified, cationic liposomes were mixed in equimolar ratio.

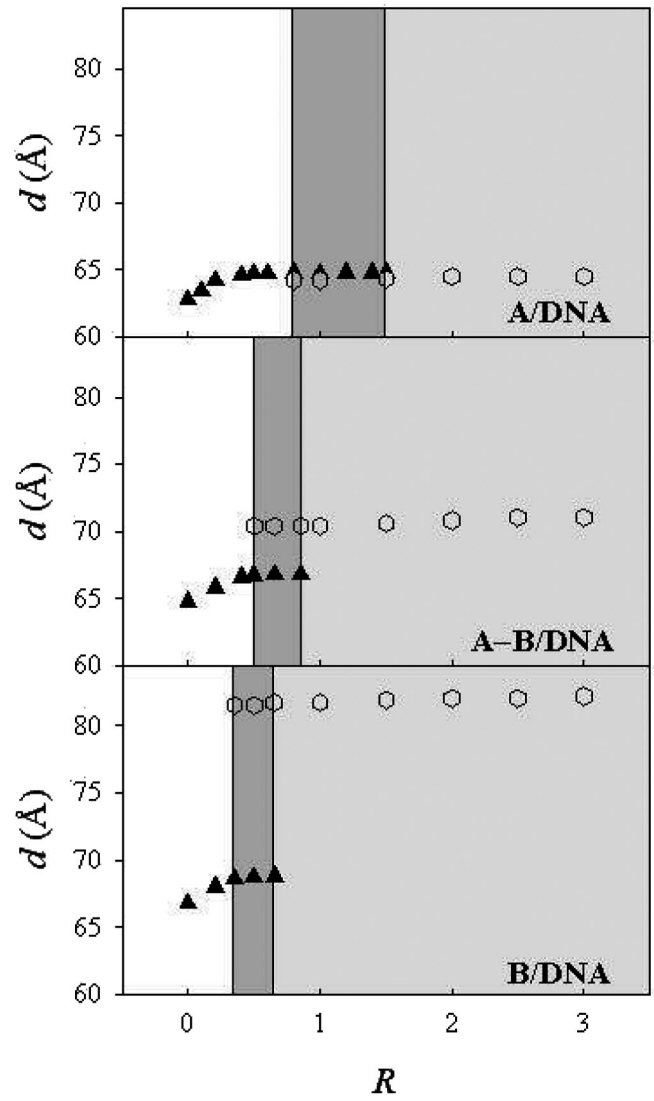

Figure 4. Phase diagram of A/DNA, A−B/DNA, and B/DNA lipoplexes with differing DOPA content. Dashed lines separate regions occupied by lamellar lipoplexes (white panel), coexisting lamellar and hexagonal lipoplexes (dark gray panel), and hexagonal lipoplexes (light gray panel). Repeat spacings, *d*, of lamellar and hexagonal lipoplexes are indicated with black triangles and white hexagons, respectively. To clarify, the *R* range was restricted to 3.5.

the physical properties of multicomponent lipoplexes are intermediate between those of binary lipoplexes and might therefore be adjusted merely by varying their lipid composition. This indicates that multicomponent lipid/DNA complexes can be prepared with designed physical properties. In the future, rationally designed vectors shall incorporate the most useful elements of synthetic systems with variations depending on their specific application.

3.3. Phase Evolution of Lipoplexes upon Interaction with Anionic Lipids. Figure 3 shows representative SAXD patterns of A/DNA/DOPA, A−B/DNA/DOPA, and B/DNA/DOPA mixtures as a function of the anionic/cationic charge ratio *R*. Here experiments with A/DNA/DOPA and B/DNA/DOPA are presented because these lipid formulations provided the clearest evidence of structural differences upon interaction with anionic lipids, while the A−B/DNA/DOPA system exhibited an intermediate behavior.

At low *R* ($R < 0.4$), only lamellar lipoplexes were found to exist with the one-dimensional (1D) DNA lattice being diluted by the anionic lipid (data not reported).[8,17,22]

As the DOPA concentration was increased in the mixture, a lamellar-hexagonal phase transition occurred. At $R = 1$, three Bragg peaks (indicated with white hexagons) were clearly visible onto the SAXD patterns of all investigated samples and were indexed as the (10), (11), and (20) reflections of an inverted hexagonal phase. Lamellar-to-hexagonal phase transition was complete at $R = 1$ in the case of both B/DNA/DOPA and A−B/DNA/DOPA systems, while A/DNA lipoplexes partly resisted solubilization as shown by the presence of the first-order lamellar Bragg peak (black triangle). The tendency to form inverted phases observed here is compatible with earlier results in the literature showing that DOPA holds the potential to promote the adoption of nonlamellar structure of phospholipids.[23] Additional weak reflections (indicated with gray diamonds) were also seen. Such reflections are characteristic of the final phase of DOPA (data elsewhere reported).[22]

At $R = 5$, lamellar lipoplexes were completely solubilized, while hexagonal complexes (white hexagons) were found to coexist with pure DOPA (gray diamonds).

Figure 4 shows the phase diagram of A/DNA/DOPA, A−B/DNA/DOPA, and B/DNA/DOPA mixtures. In the white panel only were lamellar lipoplexes detected (lamellar *d* spacings are

indicated with black triangles). In the dark gray panel, lamellar and hexagonal lipoplexes coexisted. The increase of both the lamellar (black triangles) and the hexagonal (white hexagons) spacings is consistent with the inclusion of DOPA molecules within A, A−B, and B membranes.[23] Lastly, in the light gray panel, only hexagonal lipoplexes were found to exist. Structure and phase behavior of all samples listed in Table 2 (not reported) was found to be intermediate between those of A/DNA and B/DNA lipoplexes.

X-ray diffraction experiments revealed a clear correlation between lipoplex formulation and the lamellar-hexagonal phase transition rate. The ranking of lamellar lipoplexes with respect to their propensity to be solubilized by DOPA was B/DNA > A−B/DNA > A/DNA. An opposite trend was recently found when lipoplexes were mixed with anionic dioleoylphosphatidylglycerol (DOPG) (data here not presented for space considerations).[24]

Our SAXD results showed that ALs with a clear propensity to form nonlamellar phases (such as DOPA) solubilize B/DNA lipoplexes (rich in DOPE that has a negative natural curvature) more easily than A/DNA lipoplexes (rich in DOPC for which the curvature is zero). Likewise, anionic lipids with a disposition to form lamellar phases (such as DOPG) express a greater ability to destroy the initial lamellar structure of A/DNA lipoplexes than that of B/DNA lipoplexes. The general meaning of our findings is that the propensity of lipoplexes to be destroyed by ALs correlates with the interfacial curvature of lipids forming lipoplexes and anionic liposomes. This is why the characteristics of lamellar lipoplexes in terms of resisting solubilization may only be meaningful in the context of specific anionic membranes. Our findings suggest that optimal transfection may be obtained by tailoring lipoplex composition to the lipid composition of target cells.

In summary, we did not find any sensible correlation between transfection efficiency (as reported in Figure 2) and structural evolution of lipoplexes when interacting with anionic cellular lipids, the main difference between lipoplex formulations being the lamellar-hexagonal phase transition rate. In principle, the phase behavior of the anionic−cationic lipid mixtures is expected to influence DNA release and, in turn, transfection efficiency. Thus, we investigated the DNA release from lipoplexes by ALs.

3.4. DNA Release from Lipoplexes Induced by ALs. The extent of DNA release from different lipoplex formulations after interaction with anionic DOPA was investigated by electrophoresis on agarose gels as a function of increasing R. The total amount of migrated DNA is the sum of two parts: DNA unprotected by CLs ($X_{DNA}(R = 0)$) plus DNA released from lipoplexes by anionic lipids $X_{DNA}(R)$. The former contribution can be measured by performing an electrophoresis experiment at $R = 0$ (i.e., with no anionic lipid added), while the latter contribution can be calculated based on the difference between total migrated DNA and X_{DNA} ($R = 0$). In Figure 5 we show the molar fraction of DNA released from differently efficient A−B/DNA and B/DNA lipoplexes by DOPA.

First, we observe that DNA starts to be released at $R \sim 0.5$ approximately when lamellar-hexagonal transition begins. Such a finding is in good agreement with the growing opinion that nonlamellar phase changes of the lipoplexes facilitated by intracellular lipids allow destabilization of endosomal membranes and promote DNA release. In Figure 6 is shown a schematic cartoon explaining the mechanism of interaction between lamellar lipoplexes and DOPA liposomes (gray). DOPA molecules diffuse within membranes, promoting a lamellar-to-hexagonal phase transition, and DNA starts to be released.

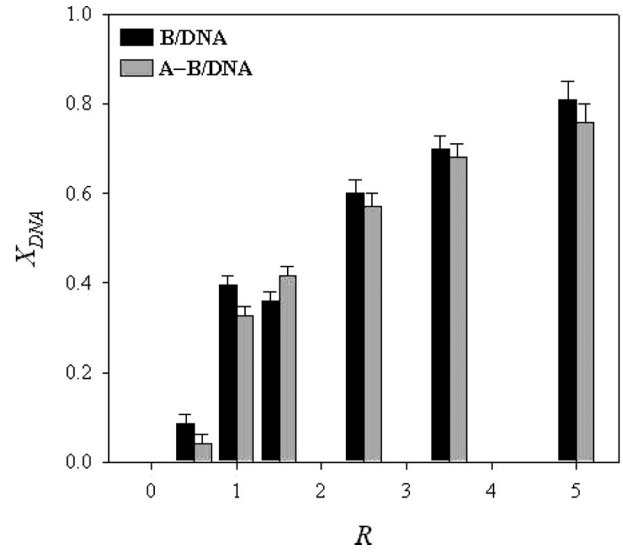

Figure 5. Molar fraction of DNA released, X_{DNA}, from B/DNA and A−B/DNA lipoplexes by ALs as a function of increasing R.

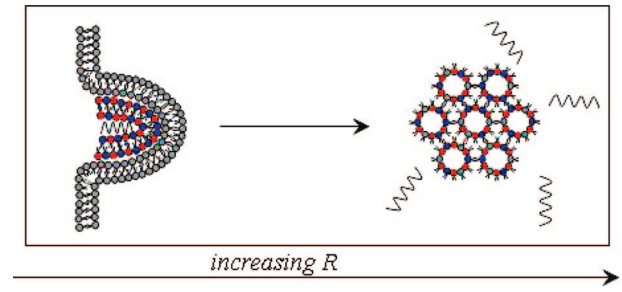

Figure 6. Schematic cartoon showing the interaction between lamellar lipoplexes and DOPA anionic liposomes (in gray). As the DOPA concentration in the mixture is increased, a lamellar-hexagonal phase transition of lipoplexes occurs and DNA starts to be released.

In addition, we observe that X_{DNA} increases with R with the profile seemingly being not dependent on lipid formulations. Thus, the superiority in transfection efficiency of a given formulation could not be explained in terms of a different extent of DNA release upon interaction with anionic lipids.

4. Discussion

Clarifying the mechanisms of lipofection is of primary importance to increase the transfection efficiency of lipoplexes. Among physical−chemical parameters affecting TE, the membrane charge density has recently been identified as a universal parameter that governs the TE behavior of lamellar lipoplexes in vitro. The purpose of this work was to investigate the TE behavior of multicomponent lipoplexes in the regime of optimal membrane charge density ($1 < \sigma_M < 2 \times 10^{-2}$ e/Å^2) and compare their performance with that of binary lipoplexes usually employed for gene delivery purposes.[6,7] Such a comparison was expected to shed light on the exact role of membrane charge density as a universal parameter for transfection by lamellar lipoplexes.

In the region of optimal charge density, the universal Gaussian curve of TE versus σ_M is expected to be poorly curved.[7] By contrast, our TE data, when plotted versus σ_M, did not exhibit such a saturated behavior but merged onto a Gaussian curve (Figure 2). We observed that a maximum in transfection was obtained when multicomponent lipoplexes where used to

transfect NIH 3T3 cells, while binary lipoplexes were definitely less efficient. This finding suggests that, at fixed σ_M, distinct levels of transfection can be obtained by adjusting other physical−chemical properties of lipoplexes such as, for instance, the number of lipid components. The general meaning of our findings is that membrane charge density controls transfection behavior of lamellar lipoplexes, with specific variations depending on lipid composition.

To provide a rationale for discrepancy between our findings[8] and those previously reported,[7] we investigated some physical−chemical features that might account for the superior transfection efficiency of the most efficient multicomponent lipoplexes such as their lipid composition, structure, propensity to be disintegrated by ALs, and ability to release DNA. All investigated lipoplexes were arranged into lamellar arrays, with distinct DNA packing densities reflecting their different membrane charge density (Table 2).

Current work shows that a major impediment to transfection involves the relative inefficient destabilization of membrane-bound compartments in which lipoplexes are confined after their internalization. A current opinion is that the structural evolution of lipoplexes upon interaction with cellular lipids may be a controlling factor in DNA release.[23,25,26] Evidence is accumulating that the lamellar/nonlamellar phase transition of lipoplexes facilitated by intracellular lipids, allowing destabilization of endosomal membranes and being helpful in plasmid translocation into the cytosol, is a prerequisite for nuclear delivery.[23,25,26]

However, after interaction with anionic DOPA vesicles, used to simulate lipoplex−endosomal membrane interaction, all tested formulations exhibited a practically identical lamellar-inverted hexagonal phase change with minor differences in transition rate (Figure 4). Thus, we were not able to correlate the propensity of a given formulation to form nonlamellar phases with distinct levels of TE.

As mentioned above, another factor that is likely to be important in the efficiency of transfection is the dissociation of DNA from cationic lipids. It appears highly critical for accomplishing efficient translocation of nucleic acids across the endosomal membrane into the cytosol for transport to the nucleus. Thus, we measured the extent of DNA release from different lipoplex formulations after interaction with ALs by electrophoresis on agarose gels as a function of increasing R.

We observe (Figure 5) that X_{DNA} does not vary significantly with R with lipid formulations. This observation correlates well with our SAXD findings showing a virtually identical phase evolution of the tested lipoplex formulations as a function of R. Indeed, we have recently shown[8,24] the existence of a strict correlation between destabilization of lipoplexes and DNA unbinding: the most stable lipoplexes display the lowest extent of DNA release, while lipoplexes with the highest propensity to be disintegrated by anionic lipids also exhibit much larger DNA release.[24]

As a result, neither the structural changes of lipoplexes upon interaction with anionic cellular lipids nor their ability to release DNA were found to correlate with TE. Apparently, parameters other than simple structural stability of lipoplexes against solubilization by ALs determined the transfection capacity of a given complex. Specifically, on the basis of observations of TE behavior of multicomponent lipoplexes in the regime of low[8] and optimal membrane charge density, our results suggest that the transfection efficiency may be strictly related to the composition of lipoplex formulations. To better test these suggestions, in Figure 7 we plotted TE as a function of both DC-Chol/DOTAP and DOPE/PC ratios. We observe that TE

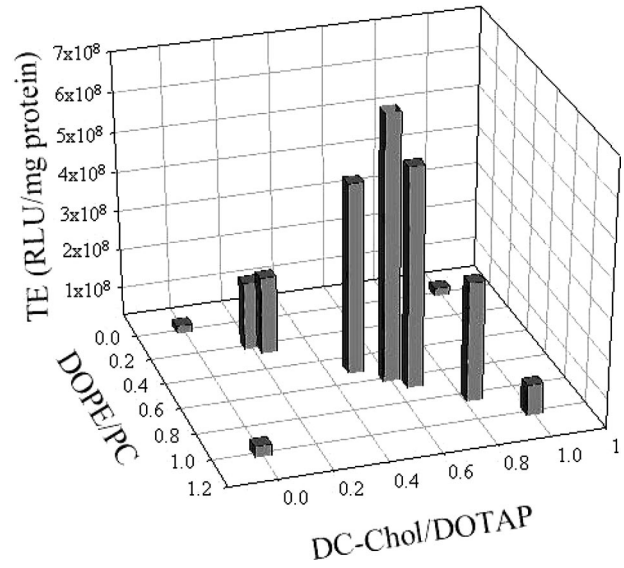

Figure 7. TE in RLU per milligram of cellular protein plotted as a function of both DC-Chol/DOTAP and DOPE/PC ratios.

peaked at DC-Chol/DOTAP = 0.5 and DOPE/PC = 0.5 when both cationic and neutral lipid species are mixed in equimolar ratio. We observed that not only the number of lipid components but also their relative molar ratio (i.e., the specific composition of the lipid carrier) altered transfection activity. First, the choice of cationic lipid can affect TE significantly. Indeed, DC-Chol-based lipoplexes (DC-Chol/DOTAP = 1) were found to be more efficient than those containing DOTAP as cationic lipid (DC-Chol/DOTAP = 0). Neutral colipids can also alter activity of lipoplexes. For instance, B/DNA lipoplexes (DC-Chol/DOTAP = 1, DOPE/PC = 1) were found to be 2-fold more efficient than D/DNA lipoplexes (DC-Chol/DOTAP = 1, DOPE/PC = 0). This finding indicates that, at a fix number of lipid components, DOPE as a colipid gave higher transfection in DC-Chol-containing lipoplexes.

Our findings add a compositional degree of freedom, because efficiently transfecting complexes can be prepared from a broad range of lipids maximizing TE if composition is optimized. The exact physical−chemical reasons why multicomponent lipoplexes are more efficient than binary lipoplexes cannot be stated unambiguously. However, some speculative arguments can be proposed. Among the barriers to transfection, escape from endosomal compartments is a major obstacle for efficient DNA delivery. The capacity of amphiphile molecules to perturb the endosomal bilayer structure will be of primary importance in facilitating the plasmid release. However, biological membranes are complex multicomponent systems consisting of mixtures of many different lipids and proteins. Accordingly, the superiority in TE of multicomponent lipoplexes may be related to the higher fusogenicity and compatibility of vesicles made of several lipid components with respect to single lipids or binary lipoplexes.[27,28] This relationship between delivery activity and physical property can be rationalized on the basis of the known consequences of packing defects as well as large local density fluctuations that could be responsible for the enhanced fusogenicity of multicomponent blends of lipids. We therefore emphasize the importance of the lipid composition of both lipoplexes and target membranes and suggest that adapting lipoplex composition to the lipid composition of target cells may be a successful strategy for the rational design of superior cationic lipid carriers. Indeed, even though the significance of lipid diversity in biological membranes still remains obscure,

it is expected to play a role in formation of nonbilayer phases, membrane interaction, and fusion and biocompatibility.[29]

5. Conclusions

In this work, we have investigated the transfection behavior of multicomponent lipoplexes in the range of optimal membrane charge density. Such complexes have presented a much higher transfection efficiency than binary lipoplexes, which are more commonly used for gene-delivery purposes. These results highlight the compositional properties of carrier lipid/cellular lipid mixtures as decisive factors for transfection and suggest that multicomponent systems are especially promising lipoplex candidates.

The biological and cellular responses to the process of physical stimulation involving gene transfer also deserve more consideration. Innovation in applying the principles of physics, chemistry, and biology to the development of a safe and effective method for gene delivery is the key to make the urgently needed advances in nonviral gene therapy. In the next future, the engineering of lipoplexes, incorporating the specific properties of different lipid species, may represent the starting point to rationally design highly specific gene vectors.

References and Notes

(1) Felgner, P. L.; Ringold, G. M. *Nature* **1989**, *337*, 387–388.
(2) Safinya, C. R. *Curr. Opin. Struct. Biol.* **2001**, *11*, 440–448.
(3) Lin, A. J.; Slack, N. L.; Ahmad, A.; Koltover, I.; George, C. X.; Samuel, C. E.; Safinya, C. R. *J. Drug Target.* **2000**, *8*, 13–27.
(4) Caracciolo, G.; Pozzi, D.; Caminiti, R.; Congiu Castellano, A. *Eur. Phys. J. E* **2003**, *10*, 331–336.
(5) McManus, J. J.; Rädler, J. O.; Dawson, K. A. *J. Am. Chem. Soc.* **2004**, *126*, 15966–15967.
(6) Ewert, K. K.; Ahmad, A.; Evans, H. M.; Safinya, C. R. *Expert Opin. Biol. Ther.* **2005**, *5*, 33–53.
(7) Ahmad, A.; Evans, H. M.; Ewert, K. K.; George, C. X.; Samuel, C. E.; Safinya, C. R. *J. Gene Med.* **2005**, *7*, 739–748.
(8) Caracciolo, G.; Marchini, C.; Pozzi, D.; Caminiti, R.; Amenitsch, H.; Montani, M.; Amici, A. *Langmuir* **2007**, *23*, 4498–4508.
(9) Caracciolo, G.; Pozzi, D.; Caminiti, R.; Amenitsch, H. *J. Phys.Chem. B* **2006**, *110*, 20829–20835.
(10) Pozzi, D.; Amenitsch, H.; Caminiti, R.; Caracciolo, G. *Chem. Phys. Lett.* **2006**, *429*, 250–254.
(11) Amenitsch, H.; Rappolt, M.; Kriechbaum, M.; Mio, H.; Laggner, P.; Bernstorff, S. *J. Synchrotron Radiat.* **1998**, *5*, 506–508.
(12) Koynova, R.; Wang, L.; Tarahovsky, Y. S.; MacDonald, R. C. *Bioconjugate Chem.* **2005**, *16*, 1335–1339.
(13) MacDonald, R. C.; Ashley, G. W.; Shida, M. M.; Rakhmanova, V. A.; Tarahovsky, Y. S.; Pantazatos, D. P.; Kennedy, M. T.; Pozharski, E. V.; Baker, K. A.; Jones, R. D.; Rosenzweig, H. S.; Choi, K. L.; Qiu, R. Z.; McIntosh, T. J. *Biophys. J.* **1999**, *77*, 2612–2629.
(14) Xu, Y. H.; Szoka, F. C. *Biochemistry* **1996**, *35*, 5616–5623.
(15) Tarahovsky, Y.; Koynova, R.; MacDonald, R. C. *Biophys. J.* **2004**, *86*, 37A.
(16) Caracciolo, G.; Pozzi, D.; Caminiti, R.; Marchini, C.; Montani, M.; Amici, A.; Amenitsch, H. *Appl. Phys. Lett.* **2006**, *89*, 233903–3.
(17) Caracciolo, G.; Pozzi, D.; Amenitsch, H.; Caminiti, R. *Langmuir* **2007**, *23*, 8713–8717.
(18) Salditt, T.; Koltover, I.; Rädler, J. O.; Safinya, C. R. *Phys. Rev. Lett.* **1997**, *79*, 2582–2585.
(19) Salditt, T.; Koltover, I.; Rädler, J. O.; Safinya, C. R. *Phys. Rev. E* **1998**, *58*, 889–904.
(20) Koltover, I.; Salditt, T.; Rädler, J. O.; Safinya, C. R. *Science* **1998**, *281*, 78–81.
(21) Artzner, F.; Zantl, R.; Rapp, G.; Rädler, J. O. *Phys. Rev. Lett.* **1998**, *81*, 5015–5018.
(22) Caracciolo, G.; Pozzi, D.; Caminiti, R.; Marchini, C.; Montani, M.; Amici, A.; Amenitsch, H. *Appl. Phys. Lett.* **2007**, *91*, 143903–3.
(23) Tarahovsky, Y. S.; Koynova, R.; MacDonald, R. C. *Biophys. J.* **2004**, *87*, 1054–1064.
(24) Caracciolo, G.; Pozzi, D.; Caminiti, R.; Marchini, C.; Montani, M.; Amici, A.; Amenitsch, H. *Biochim. Biophys. Acta* **2007**, *1768*, 2280–2292.
(25) Koynova, R.; Wang, L.; MacDonald, R. C. *Proc. Natl. Acad. Sci. U.S.A.* **2006**, *103*, 14373–14378.
(26) Wang, L.; Koynova, R.; Parikh, H.; MacDonald, R. C. *Biophys. J.* **2006**, *91*, 3692–3706.
(27) Lin, W.; Blanchette, C. D.; Longo, M. L. *Biophys. J.* **2007**, *92*, 2831–2841.
(28) Alonso, M. A.; Millán, J. *J. Cell Sci.* **2001**, *114*, 3957–3965.
(29) Pautot, S.; Frisken, B. J.; Weitz, D. A. *Proc. Natl. Acad. Sci. U.S.A.* **2003**, *100*, 10718–10721.
(30) Hed, G.; Safran, S. A. *Phys. Rev. Lett.* **2004**, *93*, 138101–4.

JP803077N